

Supplementary Online Content

Jacobson SG, Cideciyan AV, Ratnakaram R et al., Gene Therapy for Leber Congenital Amaurosis caused by *RPE65* mutations: Safety and Efficacy in Fifteen Children and Adults Followed up to Three Years.

eMethods

eComment

eTables

eReferences

eFigure Legends and eFigures 1 and 2

This supplementary material has been provided by the authors to give readers additional information about their work.

eMethods

IMMUNOLOGY PARAMETERS

Anti-AAV2 antibody titers. Serum samples from the patients were assayed for circulating antibodies to AAV2 capsid proteins as previously described¹. Briefly, 96-well plates were coated with 1.2×10^9 AAV2 particles per well overnight, then washed, blocked with 10% fetal bovine serum, and washed again. Patient serum samples and a known positive human standard were then diluted between 1:10 and 1:10,240 and allowed to bind overnight with each sample run in duplicate. Antibody detection was achieved by incubation with goat anti-human immunoglobulin detection antibody at a dilution of 1:50,000 (Biosource International/Invitrogen, Camarillo, CA) and reaction with tetramethylbenzidine peroxidase detection substrate with reading at 450 nm in an ELISA plate reader (Molecular Devices, Sunnyvale, CA). Sample anti-AAV2 titers were then determined relative to a human standard curve derived from the same plate.

Antigen-specific response. Anti-AAV2 antigen-specific lymphocyte proliferation responses were assessed as previously described¹. After isolation and purification from blood, lymphocytes were cultured at 1×10^5 cells per well of 96-well plates. Lymphocytes were separated into four groups with three control and six patient sample cultures per group: unstimulated (as negative control), stimulated with AAV2 (5,000, 500 and 50 particles/cell). After 5 days of incubation the stimulation index (SI), defined as the mean counts per minute of [³H]thymidine from stimulated cells divided by the mean counts per minute of [³H]thymidine from unstimulated cells. On the basis of previous, nonocular antigen-specific lymphocyte proliferation responses, SI values greater than 2.0-3.0 are considered significant. The viability of each lymphocyte culture was confirmed by positive controls with mitogen-induced proliferation in response to phytohemagglutinin (PHA) and recall antigen induced proliferation to *Candida albicans*.

AAV DNA in peripheral blood. Biodistribution of AAV DNA were assessed as previously described¹. In brief, 1 μ g of extracted genomic DNA was used in all quantitative PCRs. PCR reaction conditions included 50 cycles of 94°C for 40 sec, 37°C for 2 min, 55°C for 4 min, and 68°C for 30 sec. Primer pairs were designed to the cytomegalovirus enhancer/chicken β -actin promoter and standard curves were established by spike-in concentrations of a plasmid DNA carrying the same promoter as the clinical trial vector (CBAT). DNA samples were assayed in triplicate. The third replicate was spiked with CBAT DNA at a ratio of 100 copies/ μ g of genomic DNA. If at least 40 copies of the spike-in DNA were detected, the DNA sample was considered acceptable for reporting

vector DNA copies. When the copy number of the vector DNA found in that sample was equal to or greater than 100 copies/ μg , the sample was considered positive and the measured copy number per microgram was reported. The sample was considered negative if less than 100 copies/ μg were present. When less than 1 μg of genomic DNA was analyzed to avoid PCR inhibitors copurifying with DNA in the extracted tissue, the spike-in copy number was reduced proportionally to maintain the 100 copies/ μg DNA ratio. Biodistribution in blood was determined at the first baseline visit and on days 1, 3, and 14 post-vector injection.

Interferon-enzyme-linked immunospot assays (ELISpot). Ex vivo ELISpot. Briefly, PBMCs were added at a density of 2×10^5 cells per well and stimulated for 18–20 hr at 37°C with peptide libraries derived from the AAV2 VP1 protein at a concentration of $2 \mu\text{g}/\text{ml}$. Media alone served as a negative control, and PHA as a positive control. In addition, responses to CEF (Mabtech, Stockholm, Sweden), which contains 23 MHC class I-restricted peptides representing T cell epitopes of viruses common in the human population (cytomegalovirus, Epstein–Barr virus, and influenza) and is able to bind to a broad range of HLA molecules, served as a positive reference for each assay. The AAV2 VP1 peptide library was divided into three pools such that pool 2A contained the first 50 peptides of AAV2 VP1, pool 2B contained peptides 51–100, and pool 2C contained peptides 101–145. Spots were counted with an ELISpot reader (AID Diagnostika, Strassberg, Germany). Peptide-specific cells were reported as spot-forming cells (SFCs) per 10^6 PBMCs. A minimum positive response to any peptide pools was arbitrarily defined as three times over background (medium alone control) and the response was more than 55 SFCs per 10^6 PBMCs. Cultured ELISpot. To detect low levels of resting AAV2-specific memory T cells, PBMCs were cultured in the presence of AAV2 peptide library (Pools A, B and C) and IL2 and IL7 cytokines. After 3 days, PBMCs were washed, fresh medium added and cells were incubated for another 3 days. After 6 days, cells were washed and kept overnight in fresh medium without any cytokine. The following day, cells were harvested and AAV2-specific T cell responses were analyzed by the ex-vivo IFN γ ELISpot described above. The same criteria used in the ex vivo ELISpot was used in the cultured ELISpot to score a sample as positive.

EFFICACY PARAMETERS

Fixation locus determination. The fixation locus of each eye at each visit was determined by video imaging the retina under invisible near-infrared (NIR) light (MP1, Nidek Incorporated, Fremont, CA)²⁻⁴. The MP1 device tracks a predefined retinal landmark with respect to the reference image to record eye movements in near-real time (25 Hz). Fixation testing was performed in fully dark-adapted eyes with a stationary target that subtended 1° diameter; the target intensity was adjustable up to ~4 log units brighter than normal (dark-adapted) foveal threshold. Fixation recordings were performed monocularly with the contralateral eye patched. Fixation data and the associated reference image were exported and registered to wide-field NIR fundus photos. The exact location of the anatomical fovea was determined from retinal thickness maps (RTVue-100; Optovue Inc., Fremont, CA) and transferred to the co-registered images. Raw fixation data were converted to horizontal and vertical offset values from the anatomical fovea and descriptive statistics of fixation behavior were calculated over a representative 10 s long epoch.

Full-field stimulus testing (FST). Full-field stimulus testing (FST) was performed using a LED-based Ganzfeld stimulator (Colordome, Diagnosys LLC, Littleton, MA)^{1,5-7}. Blue and red stimuli were used for testing monocularly under two dark adapted conditions: standard dark adaptation of <2 hours and extended dark adaptation of >3 hours. Under each adaptation condition, the sensitivity difference between blue and red stimuli allowed estimation of which photoreceptor type was mediating the response. For blue flashes, only extended dark adaptation results are reported. For red flashes, extended dark adaptation results are reported if they were mediated by cones; otherwise, standard dark adaptation results are reported and these were always mediated by cones in RPE65-LCA eyes. Baseline data were collected at two pre-treatment visits obtained on different days within one week before surgery. Two additional pre-treatment visits on different days were available for all patients within 1 to 13 months preceding the surgery. Post-treatment data were obtained for as long as 3 years in Cohort 1; the minimum follow-up was 1 month in P15 of Cohort 5. FST sensitivity change was defined as the signed difference between each session and the mean baseline sensitivity for each eye; a positive change indicates improvement. Test-retest variability of this technique has been published^{5,6}.

Dark-adapted static visual field testing. A modified automated perimeter (Humphrey Field Analyzer; Zeiss Meditec Inc, Dublin, CA) was used to present achromatic (white)

stimuli (1.7° diameter; 200 ms duration) in the dark on a 12° grid across the visual field; the central field was also examined (at 2° intervals) using vertical and horizontal profiles^{3,4,8,9}. For the analysis, sensitivity change was defined as the locus-specific difference of sensitivity between baseline and postoperative values. Sensitivity changes of ≥8 dB were considered significant, based on our published test-retest variability testing in this patient population^{3,4}. To summarize the data, we determined the sensitivity change at all loci and at each postoperative timepoint and constructed maps of loci with significant change. Due to staggered patient enrollment, early cohorts had at least 2 years of follow-up while the last cohort was between 90 and 30 days. For Cohorts 1-4, we determined which loci showed significant increases at 3 or more postoperative visits. From these data, visual field maps were developed of the site(s) of the increase. For Cohort 5, we used 1 or more visits with significantly increased sensitivity postoperatively to develop the maps.

Transient pupillary light reflex (TPLR): Direct TPLR was elicited with short duration (100 ms) light stimuli spanning a dynamic range of ~9 log₁₀ units in the dark-adapted state^{3,7,10}. The light stimulated pupil was imaged with an infrared-sensitive video camera and digitized to estimate the pupil diameter as a function of time after stimulus presentation. TPLR amplitude was defined as the difference between the pupil diameter at a fixed time (0.9 s) after the onset of the stimulus and the pre-stimulus baseline. Luminance-response functions were derived from TPLR amplitude to increasing intensities (from -6.6 to 2.3 log scot-cd.m⁻²) of green stimuli. TPLR response threshold was defined as the stimulus luminance that evoked a criterion (0.3 mm, limit of spontaneous oscillations in pupil diameter^{3,10}) contraction of the pupil diameter at the fixed time (0.9 s) considered. TPLR sensitivity is reported as the reciprocal of the TPLR response threshold.

Mobility performance task. An indoor obstacle course¹¹⁻¹⁶ was built in a large room (4.6 X 2.7 m). 17 light-colored styrofoam wall segments (2.4 X 0.6 m) were suspended from wire tracks below ceiling level that crossed the room every 1.4 m. The wall segments were tethered only at ceiling level and were able to be shifted along the wire track to any of 4 positions. Floor-level obstacles were also part of the course and consisted of light-colored 0.6 m high objects that could be moved to various locations along the course. All obstacles were designed to fall away from the patient if touched and thus not to be hazardous. The patient was guided by an investigator from an anteroom into the mobility course area and instructed to walk forward from a starting point through the course to

the far end of the room and to try to avoid any obstacles encountered en route. The study occurred after extended dark adaptation. There were three trials for each eye at each of 5 levels of ambient room illumination (0.2, 0.6, 2, 4 and 100 lux) always beginning at the lowest level and proceeding to the highest. Using a pseudo-random sequence, changes were made in the course (from 12 possible combinations of wall and obstacle positions) between each of the 39 trials. The number of patient incidents (bumps to obstacles and walls; reorientations) per trial was noted. The average number of incidents was calculated for each illumination level by dividing the total number of incidents by the number of trials. Performance differences were determined by comparing the average number of incidents at postoperative visits and baseline. Interocular differences (IODs) were obtained by comparing the average number of incidents for control eyes with those of study eyes. Postoperative IODs were obtained by averaging IODs across all postoperative visits. Summary statistics were obtained for postoperative IODs and their distribution was illustrated with frequency histograms.

***In vivo* Bioassay for Biological Activity of Vector**

Naturally-occurring *Rpe65*-mutant *rd12* mice (n=86) were used as a bioassay for the residual vector after each human surgery. Procedures were conducted in accordance with the ARVO Statement for the Use of Animals in Ophthalmic and Visual Research and with institutional approval. Breeding, origins, maintenance before and after surgery and surgical details have been described^{17,18}. A single 1 μ l subretinal injection of the vector which remained in the syringe after each human surgery was delivered subretinally to one eye of *rd12* mice (ages 17-52 days; n=4-9 mice per patient surgery). Uninjected eyes of the same animals served as controls. ERG recordings were performed 25-37 days after the injection. In brief, full field bilateral ERGs were recorded as described^{3,18}. Animals were dark-adapted (>12 h) and anesthetized with intramuscular ketamine HCl (65 mg/kg) and xylazine (5 mg/kg); corneas were anesthetized with proparacaine HCl, and pupils dilated with tropicamide (1%) and phenylephrine (2.5%). Responses evoked by a 0.1 log scot-cd.s.m⁻² flash were amplified, filtered (-3 dB cutoff at 0.3 and 300 Hz) and digitized (2 kHz) with a 12-bit analog-to-digital converter. B-wave amplitudes were measured conventionally, from baseline or a-wave trough to positive peak, and vector-injected eyes were plotted against uninjected fellow eyes. Existence of a statistically significant efficacy due to vector was defined in each animal by comparison to the expected variability (3SD) of

interocular differences (IOD) of this waveform amplitude in untreated *rd12* and wild-type eyes^{3,18}.

eComment

The advantages of treating RPE65-LCA

RPE65-LCA has proven to be a fortuitous choice of human disease with which to begin human ocular gene therapy trials for inherited retinopathies. Obvious advantages were the accumulated basic science knowledge of the visual cycle, understanding of the *RPE65* gene and its role in the biochemical pathway, and the availability of large and small animal models of *RPE65* deficiency for proof-of-concept experiments (reviewed in¹⁹). In addition, there existed a viral vector with a wide safety margin and capacity to carry this gene; and sufficient advances of subretinal surgery to permit the injection procedure to occur. Less acknowledged as advantageous is that *RPE65-LCA* is one of very few retinal degenerative diseases with visual dysfunction that is orders of magnitude greater than expected from partial loss of photoreceptors²⁰. Most inherited retinal degenerations have a predictable relationship of photoreceptor function and structure based on an idealized model where loss of function is related to ONL thinning^{3,20}. In *RPE65-LCA*, there was an enhanced possibility that gene therapy would lead to notable increases in vision, even if affecting a limited population of photoreceptors. Efficacy thus became the most publicized feature of these safety trials; prior to this, increased vision after a treatment attempt for inherited retinal degeneration was almost unheard of²¹. The only other treatment trials showing increased vision are reports of efficacy from electronic prostheses^{22,23}. Also, one of ten patients with retinal degeneration showed improved visual acuity post-treatment with a CNTF (ciliary neurotrophic factor)-secreting implant²⁴. The severe visual insensitivity in *RPE65-LCA* patients also can have the disadvantage of masking patchy or diffuse photoreceptor injury due to the treatment procedure. Negative effects would have to be determined by serial and quantitative OCT measurements over wide areas of retina and over prolonged periods of time, and this has not occurred in any trial reports to date.

Are there other inherited retinal degenerations that share the advantageous feature of *RPE65-LCA*, namely the potential for dramatic efficacy? The only human studies of function-structure relationship in degenerations suggesting disproportionate dysfunction to structure are of the *CEP290* (NPHP6) and *IQCB1* (NPHP5) forms of LCA and this dissociation is present in the fovea only^{25,26}. The many other autosomal recessive or X-linked recessive retinal degenerations that theoretically would be amenable to gene augmentation would be expected to show the relationship of pure

photoreceptor degenerations based on the idealized model. Depending on exact mechanism, the anticipated outcome for these conditions would be slowed or halted degeneration but if outer segments were rebuilt, there may also be improved vision.

eTables

eTable 1. AAV2 Lymphocyte Stimulation Indices (SI) at Baseline and Post-Treatment Timepoints

	SI Values					
	Baseline	Day 14	Day 90	Year 1	Year 2	Year 3
Cohort 1						
P1	1.62	1.19	1.68	2.02	nd ^a	nd
P2 ^b	1.89	0.98	2.10	1.89	nd ^a	0.54
P3	1.37	0.60	1.47	1.19	nd ^a	0.81
Cohort 2						
P4	2.61	2.10	1.43	0.62	0.86	...
P5	1.21	1.61	1.32	1.66	0.75	...
P6 ^c	1.68	1.28	1.16	0.71	0.52	...
Cohort 3						
P7	2.02	0.86	1.14	0.70
P8	NVD	0.84	1.00	0.34
P9	0.56	1.11	1.68	0.31
Cohort 4						
P10	0.69	1.03	0.75
P11	0.84	0.42	0.45
Cohort 5						
P12	0.60	1.40	0.22
P13	1.56	0.51	0.83
P14	0.49	0.96
P15

Abbreviation: Ellipses, testing not yet performed; nd, not done; NVD, no valid data.

^aTesting at Year 2 timepoint was added to protocol after Cohort 1 had already completed this timepoint.

^bP2 had extra titer performed at day 270 (1.17).

^cP6 had an extra titer performed at day 60 (1.25).

eTable 2. Ex vivo AAV2 Peptide Stimulated IFN- γ Elispot Results at Baseline and Post-Treatment Timepoints
Spot-Forming Cells (SFCs) per 10⁶ PBMCs

	Timepoint	Spot-Forming Cells (SFCs) per 10 ⁶ PBMCs				
		Medium	2A	2B	2C	CEF
Cohort 1						
P1 ^a	Baseline	28	48	40	30	143
	Day 14	20	23	13	18	228
	Day 90	15	20	15	20	158
P2	Baseline	5	3	0	3	10
	Day 14	3	0	13	3	5
	Day 90	10	15	8	8	18
	Year 3	0	3	3	10	10
P3	Baseline	23	23	18	28	1423
	Day 14	20	13	10	5	1268
	Day 90	15	10	25	30	1943
	Year 3	605	590	690	575	1960
Cohort 2						
P4	Baseline	130	73	118	70	168
	Day 14	8	13	30	25	100
	Day 90	80	80	83	80	193
	Year 2	HB	HB	HB	HB	HB
P5	Baseline	10	8	0	10	305
	Day 14	3	18	20	5	360
	Day 90	5	8	5	5	495
	Year 2	3	0	3	5	988
P6	Baseline	10	10	10	10	75
	Day 14	50	50	70	70	183
	Day 90	20	23	20	20	163
	Year 2	5	0	3	10	58
Cohort 3						
P7 ^b	Baseline	0	18	5	0	708
	Day 14	0	23	5	5	763
	Day 90	10	38	20	13	1165
P8	Baseline	10	5	10	10	55
	Day 14	5	13	8	8	45
	Day 90	25	13	18	25	63
	Year 1	10	20	20	8	55
P9	Baseline	23	20	40	30	1902
	Day 14	8	15	20	23	1135
	Day 90	18	35	35	72	2850
	Year 1	5	13	23	10	2020
Cohort 4						
P10	Baseline	5	7	15	0	25
	Day 14	40	35	45	28	58
	Day 90	5	23	7	13	23
P11	Baseline	3	5	5	3	13
	Day 14	10	3	25	23	32
	Day 90	5	45	10	20	240
Cohort 5						
P12	Baseline	3	13	28	18	378
	Day 14	HB	HB	HB	HB	HB
	Day 90	3	10	20	20	368
P13	Baseline	0	8	0	8	3
	Day 14	0	0	0	0	0
	Day 90	7	0	3	3	15
P14	Baseline	0	13	0	5	20
	Day 14	5	8	0	5	28
	Day 90	3	3	3	10	35
P15	Baseline	5	13	5	5	163
	Day 14	953	960	935	915	970

Abbreviations: Ellipses, testing not yet performed; HB, high background.

^aYear 3 testing not performed in P1.

^bYear 1 testing not performed in P7 because testing at this timepoint was added after the patient had completed the timepoint.

eTable 3. Cultured AAV2 Peptide Cultured IFN- γ Elispot Results at Baseline and Post-Treatment Timepoints

		Spot-Forming Cells (SFCs) per 10 ⁶ PBMCs			
	Timepoint	Medium	2A	2B	2C
Cohort 1					
P1 ^a	Baseline	943	1158	1060	1355
	Day 14	818	1228	1435	1260
	Day 90	430	778	893	675
P2	Baseline	348	1060	1015	580
	Day 14	110	620	558	433
	Day 90	195	423	365	230
P3	Year 3	25	343	275	138
	Baseline	895	1168	1335	1303
	Day 14	250	563	543	363
	Day 90	438	873	1020	1013
	Year 3	55	20	50	75
Cohort 2					
P4	Baseline	838	953	1045	1145
	Day 14	363	578	763	675
	Day 90	2040	2465	2710	2550
	Year 2	1030	1110	1320	995
P5	Baseline	183	303	520	243
	Day 14	140	500	915	675
	Day 90	360	870	1080	675
	Year 2	188	265	335	523
P6	Baseline	160	810	1255	1070
	Day 14 ^b	1150	2320	2210	2255
	Day 90	1450	2005	2505	2255
	Year 2	148	243	458	423
Cohort 3					
P7 ^c	Baseline	10	40	60	30
	Day 14	30	73	73	40
	Day 90	13	98	50	53
P8	Baseline	1310	2480	243	2025
	Day 14	845	1170	1530	1015
	Day 90	580	1123	1350	1590
	Year 1	635	680	1200	1520
P9	Baseline	5	120	150	178
	Day 14	10	23	30	98
	Day 90	18	203	185	298
	Year 1	33	515	603	380
Cohort 4					
P10	Baseline	13	28	18	10
	Day 14	300	875	673	743
	Day 90	173	483	493	470
P11	Baseline	43	75	223	503
	Day 14	nd	nd	nd	nd
	Day 90	60	167	440	293
Cohort 5					
P12	Baseline	190	793	825	788
	Day 14	288	245	335	340
	Day 90	295	1550	1750	1500
P13	Baseline	85	228	243	415
	Day 14	nd	nd	nd	nd
	Day 90	50	188	218	328
P14	Baseline	63	445	560	698
	Day 14	nd	nd	nd	nd
	Day 90	53	333	240	413
P15	Baseline	nd	nd	nd	nd
	Day 14	nd	nd	nd	nd

Abbreviations: Ellipses, testing not yet performed; HB, high background; ND, not done due to lack of cells. Bold values indicate positive results.

^aYear 3 testing not performed in P1.

^bTesting performed at day 30 visit because of high background on day 14 sample.

^cYear 1 testing not performed in P7 because testing at this timepoint was added after the patient had completed the timepoint.

References

1. Hauswirth WW, Aleman TS, Kaushal S, et al. Treatment of Leber congenital amaurosis due to RPE65 mutations by ocular subretinal injection of adeno-associated virus gene vector: short-term results of a phase I trial. *Hum Gene Ther.* 2008;19(10):979-990.
2. Jacobson SG, Aleman TS, Cideciyan AV, et al. Human cone photoreceptor dependence on RPE65 isomerase. *Proc Natl Acad Sci USA.* 2007;104(38):15123-15128.
3. Cideciyan AV, Aleman TS, Boye SL, et al. Human gene therapy for RPE65 isomerase deficiency activates the retinoid cycle of vision but with slow rod kinetics. *Proc Natl Acad Sci USA.* 2008;105(39):15112-15117.
4. Cideciyan AV, Hauswirth WW, Aleman TS, et al. Human RPE65 gene therapy for Leber congenital amaurosis: persistence of early visual improvements and safety at 1 year. *Hum Gene Ther.* 2009;20(9):999-1004.
5. Roman AJ, Schwartz SB, Aleman TS, et al. Quantifying rod photoreceptor-mediated vision in retinal degenerations: dark-adapted thresholds as outcome measures. *Exp Eye Res.* 2005;80(2):259-272.
6. Roman AJ, Cideciyan AV, Aleman TS, Jacobson SG. Full-field stimulus testing (FST) to quantify visual perception in severely blind candidates for treatment trials. *Physiol Meas.* 2007;28(8):N51-N56.
7. Aguirre GK, Komáromy AM, Cideciyan AV, et al. Canine and human visual cortex intact and responsive despite early retinal blindness from RPE65 mutation. *PLoS Med.* 2007;4(6):e230.
8. Jacobson SG, Voigt WJ, Parel JM, et al. Automated light- and dark-adapted perimetry for evaluating retinitis pigmentosa. *Ophthalmology.* 1986;93(12):1604-1611.
9. Jacobson SG, Aleman TS, Cideciyan AV, et al. Defining the residual vision in leber congenital amaurosis caused by RPE65 mutations. *Invest Ophthalmol Vis Sci.* 2009;50(5):2368-2375.
10. Aleman TS, Jacobson SG, et al. Impairment of the transient pupillary light reflex in Rpe65(-/-) mice and humans with leber congenital amaurosis. *Invest Ophthalmol Vis Sci.* 2004;45(4):1259-1271.
11. Haymes S, Guest D, Heyes A, Johnston A. Comparison of functional mobility performance with clinical vision measures in simulated retinitis pigmentosa. *Optom Vis Sci.* 1994;71(7):442-453.
12. Geruschat DR, Turano KA, Stahl JW. Traditional measures of mobility performance and retinitis pigmentosa. *Optom Vis Sci.* 1998;75(7):525-537.
13. Turano KA, Broman AT, Bandeen-Roche K, et al. Association of visual field loss and mobility performance in older adults: Salisbury Eye Evaluation Study. *Optom Vis Sci.* 2004;81(5):298-307.
14. Hartong DT, Jorritsma FF, Neve JJ, Melis-Dankers BJ, Kooijman AC. Improved mobility and independence of night-blind people using night-vision goggles. *Invest Ophthalmol Vis Sci.* 2004;45(6):1725-1731.
15. Leat SJ, Lovie-Kitchin JE. Measuring mobility performance: experience gained in designing a mobility course. *Clin Exp Optom.* 2006;89(4):215-228.
16. Rubin GS, Bainbridge JW, Roche, et al. Visually-guided mobility in patients treated with gene therapy for leber's congenital amaurosis. *Invest Ophthalmol Vis Sci.* 2010;51: E-Abstract 1392.
17. Pang JJ, Chang B, Hawes NL, et al. Retinal degeneration 12 (rd12): a new, spontaneously arising mouse model for human Leber congenital amaurosis (LCA). *Mol Vis.* 2005;11:152-162.
18. Roman AJ, Boye SL, Aleman TS, Pang JJ, et al. Electroretinographic analyses of Rpe65-mutant rd12 mice: developing an in vivo bioassay for human gene therapy trials of Leber congenital amaurosis. *Mol Vis.* 2007;13:1701-1710.
19. Cideciyan AV. Leber congenital amaurosis due to RPE65 mutations and its treatment with gene therapy. *Prog Retin Eye Res.* 2010;29(5):398-427.
20. Jacobson SG, Aleman TS, Cideciyan AV, et al. Identifying photoreceptors in blind eyes caused by RPE65 mutations: Prerequisite for human gene therapy success. *Proc Natl Acad Sci USA.* 2005;102(17):6177-6182.
21. Jacobson SG, Cideciyan AV. Treatment possibilities for retinitis pigmentosa. *N Engl J Med.* 2010;363(17):1669-1671.
22. Freeman DK, Rizzo JF, Fried SI. Encoding visual information in retinal ganglion cells with prosthetic stimulation. *J Neural Eng.* 2011;8(3):035005. Epub 2011 May 18.

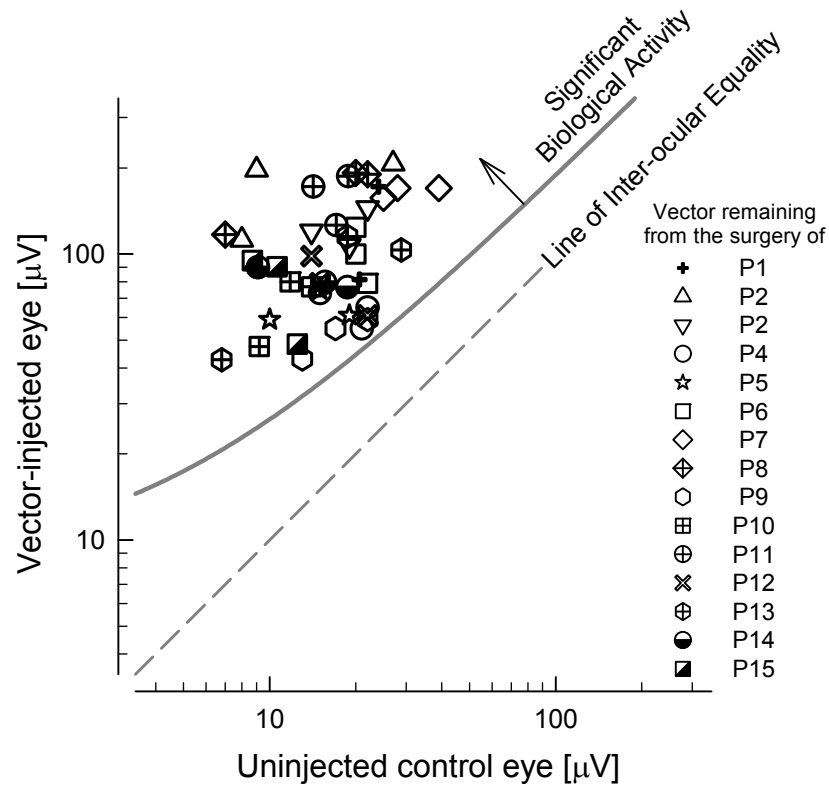
23. Chader GJ, Weiland J, Humayun MS. Artificial vision: needs, functioning, and testing of a retinal electronic prosthesis. *Prog Brain Res.* 2009;175:317-32.
24. Sieving PA, Caruso RC, Tao W, et al. Ciliary neurotrophic factor (CNTF) for human retinal degeneration : phase I trial of CNTF delivered by encapsulated cell intraocular implants. *Proc Natl Acad Sci USA.* 2006;103(10):3896-3901.
25. Cideciyan AV, Aleman TS, Jacobson SG, et al. Centrosomal-ciliary gene CEP290/NPHP6 mutations result in blindness with unexpected sparing of photoreceptors and visual brain: implications for therapy of Leber congenital amaurosis. *Hum Mutat.* 2007;28(11):1074-1083.
26. Cideciyan AV, Rachel RA, Aleman TS, et al. Cone photoreceptors are the main targets for gene therapy of NPHP5 (IQCB1) or NPHP6 (CEP290) blindness: generation of an all-cone Nphp6 hypomorph mouse that mimics the human retinal ciliopathy. *Hum Mol Genet.* 2011;20(7):1411-1423.

eFigure Legends

eFigure 1. *In vivo* bioassay of the gene therapy vector used in human *RPE65*-LCA surgery. Electroretinographic (ERG) b-wave amplitudes in vector-injected eyes of *rd12* (*Rpe65*-deficient) mice are plotted as a function of amplitudes in uninjected control eyes. Dashed line of equality corresponds to no interocular difference in this ERG parameter. A significant interocular difference (3 standard deviations, derived from untreated *rd12* and wild-type animals) is defined by the solid gray line. Figure shows results from 3 highest responding animals for each patient's vector. Significant ERG improvements provide evidence of the biologic activity of the vector used for each patient over the three year duration of the clinical trial.

eFigure 2. Rod and cone mediated visual function results based on chromatic FST in control and study eyes at baseline and all postoperative timepoints. (Note, this graph expands upon data shown in Figure 2A,B). A, FST sensitivity (mean \pm SD) to blue and red stimuli measured under dark-adapted conditions in each eye of each subject at four baseline visits (white bars) and all postoperative visits to date (black bars). For the blue stimulus, normal range mediated by rod (R) system is shown. For the red stimulus, normal ranges mediated by the cone (C) systems recorded during the cone plateau period following a bright adapting light are shown in addition to the range mediated by the R system. B, Changes in sensitivity from mean baseline shown for the blue FST stimulus in control and study eyes. The magnitude of the differences to chromatic stimuli define whether R or C systems mediate sensitivity at a given visit. R/C refers to the cases when some visits were mediated by the R system and some visits by the C system. Study and control eyes at baseline, and control eyes at the postoperative timepoints show sensitivity to the blue FST stimulus mediated by rod or cone systems. Study eyes at postoperative periods show highly significantly increases in sensitivity mediated by the rod system in all patients except one. C, Changes in sensitivity from mean baseline shown for the red FST stimulus in control and study eyes. Sensitivity to the red stimulus is mediated by the C system in all eyes at all timepoints. Highly significant increases in red FST sensitivity demonstrate improvement of cone function postoperatively.

BIOLOGICAL ACTIVITY OF VECTOR INJECTED USING AN ERG ASSAY IN *Rd12* MICE



FULL-FIELD SENSITIVITY TESTING (FST)

